Analyst

PAPER

View Article Online
View Journal | View Issue

Cite this: *Analyst*, 2025, **150**, 5201

Optimisation of electron-induced dissociation parameters for molecular annotation of glycerides and phospholipids in fast LC-MS

Vincen Wu,[a] Abraham Moyal,[a] Alaa Othman†[a] and Nicola Zamboni *[a,b]

Electron-induced dissociation methods, particularly electron impact excitation of ions from organics (EIEIO), offer enhanced capabilities for lipid structural elucidation over traditional collision-induced dissociation (CID). Despite their analytical promise, the practicality of EIEIO within routine liquid chromatography-mass spectrometry (LC-MS) workflows remains largely unexplored. In this study, we optimised LC-EIEIO-MS analysis for the rapid and detailed structural annotation of glycerides and phospholipids. We evaluated the effects of reaction times, accumulation times, and electron kinetic energies using lipid standards from multiple classes and at varying concentrations. Our results revealed that short reaction times of 30 ms consistently yielded stronger diagnostic signals crucial for lipid class identification and *sn*-position discrimination at concentrations as low as 200 pg on column. To systematically infer the position of double bonds from EIEIO spectra, we introduced LipidOracle, a software that tests all possible isomers and correctly accounts for missing data, noise, and crowded spectra. We demonstrated that longer accumulation times of 200 ms were most effective for determining carbon–carbon double bond (C=C) positions, particularly in polyunsaturated lipids. Finally, we evaluated the performance of EIEIO with liver and plasma extracts. Overall, we demonstrate that comprehensive lipid structural characterisation, including *sn*-position and double bond locations in fatty acyl chains, is achievable within typical LC-MS timescales (~0.2 s). Our findings outline practical guidelines for high-throughput analysis of complex lipid samples by EIEIO.

Received 22nd May 2025,
Accepted 17th October 2025

DOI: 10.1039/d5an00567a

rsc.li/analyst

Introduction

Lipidomics has emerged as a powerful field for profiling the myriad lipid species in biological systems, enabled by advances in high-resolution LC-MS technologies.[1,2] Lipids exhibit enormous structural diversity – varying in headgroup classes, fatty acyl chain lengths, positions of unsaturation, stereochemistry, oxidation, *etc.* – which underlies their diverse biological functions in membranes, energy storage, and signaling.[3,4] However, comprehensive structural elucidation of lipids remains challenging. In typical workflows, tandem mass spectrometry of lipids is dominated by collision-induced dissociation (CID), which readily provides the lipid class and total fatty acyl composition but often cannot distinguish isomeric details such as the regiospecific (*sn*) positions of acyl chains or the location of carbon–carbon double bonds.[5] The inability to resolve such isomeric structures can impede a full understanding of lipid biology; for example, failing to differentiate positional isomers may preclude definitive biomarker identification or accurate mapping of metabolic pathways.[6]

To overcome these limitations, several approaches of chemical modification and alternative dissociation techniques have been developed to obtain additional structural information by enhancing fragmentation in the proximity of carbon double bonds or in the glycerol backbone. For example, the Paternò–Büchi reaction uses UV irradiation to induce the formation of an oxetane ring in the place of a carbon double bond, which then can be readily fragmented with CID.[7] A similar result can be obtained with the previous aziridination of carbon–carbon double bonds in solution and LC-MS/MS analysis with CID.[8,9] For practical reasons, there is considerable interest in methods that can be performed online in MS instruments on gas-phase ions. A prominent method is ozone-induced dissociation (OzID), which exploits the reactivity of ozone to selectively cleave lipid double bonds, generating fragment ions that reveal the positions of unsaturation.[10,11] Equivalent diagnostic fragments can be obtained by exposing transiting ions to oxygen radicals in oxygen attachment dissociation (OAD).[12,13] The alternative is to activate gas-phase

[a]*ETH Zurich, Institute of Molecular Systems Biology, Zurich, Switzerland.*
E-mail: zamboni@imsb.biol.ethz.ch
[b]*PHRT Swiss Multi-Omics Center, Zurich, Switzerland*
† Current address: Functional Genomics Center Zurich, Switzerland.

ions with photons or electrons. For example, ultraviolet photodissociation (UVPD), in particular at a wavelength of 193 nm, fragments both double bonds in acyl chains as well as the backbone.[14] Commercial UVPD mass spectrometers, however, mount a 213 nm laser that, in our experience, requires longer excitation and acquisition time of 200 ms and longer for most species, and are hard to apply in untargeted workflows.

Electron-mediated fragmentation techniques have also gained attention for comprehensive lipid structural analysis. In particular, electron impact excitation of ions from organics (EIEIO) involves bombarding singly charged ions with electrons of low kinetic energy (~8–15 eV). In lipids, EIEIO induces a rich array of radical-driven cleavages, including the major diagnostic fragments commonly obtained by CID and additional cleavages that allow for the identification of the position of C=C bonds in acyl chains or for the discrimination of fatty acyl regiochemistry. The added value provided by EIEIO has been widely demonstrated by seminal work by Baba and his collaborators. Both for glycerophospholipids and triglycerides,[15–18] they achieved nearly complete structural elucidation in a single EIEIO MS^2 spectrum, missing only the stereochemical elucidation of *cis*-/*trans*-conformation at double bonds. These studies, however, were done under ideal conditions using highly concentrated solutions of pure standards and direct infusion to collect MS^2 data for up to 20 min to obtain possibly clean EIEIO spectra. This was necessary because most EIEIO-specific fragments, particularly those associated with cleavages of the acyl chains, are 2–3 orders of magnitude less intense than the common fragments from the headgroup.

Here we address whether EIEIO-based fragmentation is compatible with untargeted LC-MS workflows, in which the acquisition of MS^2 data for a single precursor can last only a fraction of a second, or much less in the case of complex samples. Using diluted standards across multiple classes of lipids and acquisition times ranging from 35 to 500 ms, we evaluated the conditions under which it is possible to acquire EIEIO data to determine either the class, regiochemistry, or position of carbon–carbon double bonds in polyunsaturated lipids. Finally, we benchmark the optimized method with the analysis of plasma and liver extracts. Our findings establish practical guidelines for incorporating EIEIO into lipidomics workflows.

Materials and methods

Chemicals

Water was obtained from a Milli-Q system. Acetonitrile, 2-propanol, and formic acid were purchased from Sigma-Aldrich (Merck, Germany). Ammonium acetate was purchased from Fisher Scientific (Thermo Fisher Scientific, USA). Lipids standards were purchased from Avanti Polar Lipids (Avanti, USA). They consisted of the LightSPLASH mix, which includes 13 primary lipid standards at a stock concentration of 100 μg mL^{-1}: PC 15:0/18:1(9*Z*), LPC 0:0/18:1(9*Z*), PE 15:0/18:1(9*Z*), LPE 0:0/18:1(9*Z*), PG 15:0/18:1(9*Z*), PI 15:0/18:1(9*Z*), PS 15:0/18:1(9*Z*), TG 15:0/18:1(9*Z*)/15:0, DG 18:1(9*Z*)/15:0/0:0, MG 18:1(9*Z*)/0:0/0:0, CE 18:1(9*Z*), SM 18:1;O2/18:1(9*Z*), Cer 18:1;O2/15:0. For tests with multiple double bonds, we included PE 18:0/20:4(5*Z*,8*Z*,11*Z*,14*Z*) and PE 18:0/22:6(4*Z*,7*Z*,10*Z*,13*Z*,16*Z*,19*Z*). For analysis, lipid standards were diluted with 2-propanol to a working concentration between 1 μg mL^{-1} and 1 ng mL^{-1}. NIST Standard Reference Material 1950 metabolites in frozen human plasma was purchased from Sigma-Aldrich (Merck, Germany). Liver extract total in chloroform was purchased from Avanti Polar Lipids (Avanti, USA).

Sample preparation

Samples were first thawed and were followed by single phase extraction protocol using only 2-propanol. Plasma lipids were extracted from 10 μL of frozen NIST SRM1950 by mixing with 300 μL 2-propanol at room temperature, followed by vortexing for 20 seconds, and 30 minutes of incubation at −20 °C. After incubation, the extract was centrifuged at 14 000 rpm for 20 minutes at 4 °C. Supernatant was transferred to HPLC vial with insert. The stock liver extract was diluted to 1 mg mL^{-1} with 2-propanol, from which 200 μL was transferred to HPLC vial with insert.

LC-MS analysis

Chromatographic separation was conducted using a 1290 Infinity II (Agilent, USA) equipped with an Acquity BEH C18 column 2.1 mm × 30 mm, 1.7 μm (Waters, USA) for the short LC method and Acquity BEH C18 column 2.1 mm × 100 mm, 1.7 μm (Waters, USA) for the long LC method at a column temperature of 60 °C. The mobile phase A consisted of acetonitrile/water (60 : 40), 0.1% formic acid, and 10 mM ammonium acetate. The mobile phase B comprised 2-propanol/acetonitrile (90 : 10), 0.1% formic acid, and 10 mM ammonium acetate. We employed two gradient profiles. The short LC method (2.5 min) commenced with an initial condition of 85% A, followed by linear gradients from 85 to 70% A (0 : 00–0.29 min), 70 to 52% A (0.29–0.37 min), 52 to 18% A (0.37–1.64 min), and 18 to 1% A (1.64–1.72 min), with a plateau at 1% A. This was succeeded by a steep gradient from 1 to 85% A (1.79–1.81 min) and equilibration at 85% A (1.81–2.24 min) (85–85% A). The long LC method (15 minutes) also began with an initial condition of 85% A, followed by slower gradients: 85 to 70% A in 2.00 min, 70 to 52% A (2.00–2.50 min), 52 to 18% A (2.50–11.00 min), 18 to 1% A (11.0–11.50 min), 0.5 min at 1%A, and concluded with equilibration at 85% A (12.10–15.00 min). The flow rate was 1.2 mL min^{-1} for the short method and 0.6 mL min^{-1} for the long method, and the injection volume was 2 μL, which resulted in loading 2 ng, 200 pg, or 20 pg of lipid standards onto the column.

Parameter optimisation was done with a SCIEX ZenoTOF 7600 System (SCIEX, Canada) in positive ionisation mode.[19] The following are the parameters for mass spectrometry during data acquisition: electrospray voltage at +5.5 kV; source temperature at 700 °C; mass range of *m*/*z* 100–1000; accumu-

lation time at 75 ms; declustering potential at 60 V; declustering potential spread at 0 V; ion source gas 1 at 70 psi; ion source gas 2 at 70 psi; curtain gas at 45 psi; CAD gas at 7 psi. The MSMS parameters were set as EAD with top 2 ions for every survey scan, excluding ion for 1 second after 1 occurrence; mass range *m*/*z* 100–1000; declustering potential at 60 V; declustering potential spread at 0 V; Zeno pulsing is turned on with Zeno threshold set at 500 000 cps; Q1 unit resolution; time bin to sum at 6 with all 4 channels selected; EAD RF set at 80 Da. Unless otherwise specified, electrons in EIEIO were generated with a current of 7500 nA and accelerated by a field of 12 eV, with variety of different reaction time and accumulation time paired together in a quasi-factorial design experiment (reaction time – accumulation time: 30 ms – 35 ms; 30 ms–120 ms; 30 ms–200 ms; 60 ms–65 ms; 60 ms–135 ms; 60 ms–200 ms; 90 ms–95 ms; 90 ms–150 ms; 90 ms–200 ms; 115 ms–120 ms; 115 ms–160 ms; 115 ms–200 ms) for the short LC method. For the 15-minute LC method, reaction times and accumulation times were paired as follows: 30 ms–35 ms, 30 ms–65 ms, 30 ms–120 ms, 30 ms–200 ms, and 30 ms–500 ms.

Additional analyses were done on the SCIEX ZenoTOF 8600 System (SCIEX, Canada) in positive ionisation mode with the following parameters: electrospray voltage at +4.5 kV; source temperature at 400 °C; mass range of *m*/*z* 50–1000; accumulation time at 250 ms; ion source gas 1 at 50 psi; ion source gas 2 at 60 psi; curtain gas at 45 psi; CAD gas at 7 psi. The MS/MS parameters were set as EAD with top 4 ions for every survey scan, excluding ion for 3 seconds after 1 occurrence; mass range *m*/*z* 50–1000; Q1 unit resolution; reaction time was set at 30 ms; accumulation time was set at 200 ms; electron kinetic energy was set at 12 eV with 7500 nA beam current; EAD RF was 80 Da; time bins to sum was set at 6.

Nomenclature

We follow the nomenclature shorthand notation of lipids according to LIPID MAPS.[20] In short, double bond positions are counted from the carboxyl end (can be denoted as Δ), whereas n- or ω- are counted from the methyl end. Geometrical isomers of double bonds are given as *Z* (*cis*) or *E* (*trans*). When *sn*-positions of acyl chains are known, acyl chains are listed in the order from *sn*-1 to 3 separated by a slash (/). An underscore indicates that the position of the acyl chains is undefined, and all permutations are equally plausible. Lipid class abbreviations are listed as follows: phosphatidylcholines (PC), lysophosphatidylcholines (LPC), phosphatidylethanolamines (PE), lysophosphatidylethanolamines (LPE), phosphatidylgylcerols (PG), phosphatidylinositols (PI), phosphatidylserines (PS), monoglycerides (MG), diglycerides (DG), triglycerides (TG), cholesteryl ester (CE), sphingomyelins (SM), ceramides (Cer). In addition, we specify the ion to indicate which adduct was isolated for MS^2 spectrum analysis. For instance, PC 16:0/18:1(9*Z*) refers to a phosphatidylcholine with a fatty acyl chain at the *sn*-1 position with 16 carbons and no double bonds, and a fatty acyl chain at the *sn*-2 position with 18 carbons and one double bond at the 9th carbon counting from the carboxyl end with *cis* geometry.

Data analysis

For the analysis of the fragments linked to the inference of lipid class and *sn*-regiochemistry, we converted the raw data mzML file with MSConvert (ProteoWizard 3.0.22291) using the vendor-provided centroiding algorithm. The resulting mzML files were processed by SLAW[21] to obtain the MGF files for all detectable features. For the analysis of double-bond position that required a precise analysis centroiding of low-abundant EIEIO peaks, we used functions provided by the Python module scipy 1.15.2. We exported profile data directly from vendor files and applied a Savitzky–Golay smoothing with a window size of 7. Peaks were detected by a local maximum procedure (find_peaks) with a minimum peak prominence of 3.0. The *m*/*z* of the centroids was refined with a local, intensity-weighted averaging. The resulting spectra were exported to MGF files and analysed by LipidOracle 0.7.36. Liver and plasma samples were processed directly from raw data using the Python package masster 0.5.17 and annotated with LipidOracle.

Lipid annotation

LipidOracle employs a two-step process for annotating each query MS^2 spectrum. In the initial step, it matches measured spectra against a library of expected MS^2 spectra, compiled with diagnostic fragments described in the literature for CID and EIEIO. The library includes permutations of *sn*-regioisomers, chain lengths, saturation levels, and oxidation states. For all variants, diagnostic fragments are included to tentatively identify the position and composition of the acyl chains. Library fragments are weighted according to their prevalence, and the matching is scored using a greedy cosine function. In this first step, for each experimental MS^2 spectrum, all matches with a score within 10% of the top match are retained, assessed individually for each spectrum. For lipids where the acyl chain composition could be determined in this step (covering 39–54% of the spectra according to Table 1), the analysis proceeds to the second step: C=C analysis. Starting with the heuristic library that provides simulated EIEIO spectra for approximately 190 000 acyl chain variants (as described in the main text), all compatible isomers are retrieved. If multiple isomers are present, combined MS^2 spectra are generated. Matching relies on a hybrid score that sums two partial scores. The first partial score measures the number of expected fragments that are matched. If all expected fragments, including H gains and losses, are matched, the partial score is 0.5. The second partial score assesses the intensity of the theoretical peaks that are matched. It gives credit for the correct identification of the V-pattern or fragments close to the ester bond. Unlike a classical dot product, the second term does not depend on the intensity of the measured EIEIO spectrum, which is often noisy and overlaid by other fragments, such as those from the head group. The maximum score for the second partial score is 0.5, and it is added to the

Table 1 Summary of lipid annotation for lipid extract of liver and human plasma (NIST SRM1950)

Sample	Liver				Plasma			
Instrument	7600		8600		7600		8600	
Features with MS^2 data	1426		2008		1004		1254	
Features with MS^2-identification	255		340		102		152	
Features with diagnostic peaks for acyl chains	130	51%	182	54%	37	36%	75	49%
Features with diagnostic peaks for *sn*-regioisomerism	49	19%	55	16%	19	19%	75	49%
Features with DB identification	88	35%	131	39%	27	26%	49	32%
Features with unique DB identification	49	19%	61	18%	17	17%	18	12%

first partial score to obtain a total score between 0 and 1. To keep only good matches, we discard all isomers with a total score below 0.5. If multiple isomers pass this threshold, we retain those within 2% of the highest total score for each query MS^2. From the final set of isomers whose predicted MS^2 spectrum best matches the query spectrum, we count how often each bond was predicted to be a C=C. For more details, refer to the online documentation at https://hub.docker.com/r/zambonilab/lipidoracle.

Results

A short reaction time is best for lipid identification

We wanted to investigate the minimum MS^2 acquisition time for obtaining meaningful structural information on glycerophospholipids by electron-associated dissociation. The shortest time we investigated was 35 ms, which results from the so-called *reaction time* of 30 ms and the additional 5 ms required to profile all fragments in the time-of-flight detector. During the reaction time, cations from the quadrupole filter are activated by a short exposure to the electron beam. The dissociation kinetics are slow, at least compared to collision-induced dissociation, and the reaction proceeds for 30 ms or longer to yield sufficient fragments. To increase the fragment yield, we tested reaction times of up to 115 ms. Fragmentation data, however, is stored based on the *accumulation time*. The shortest accumulation time is the reaction time plus the 5 ms detection time. The accumulation time can be increased to perform multiple cycles of electron activation and reaction on subsequent packets of ions, eventually obtaining a summed spectrum with improved signal-to-noise. Increasing both the reaction time and the number of cycles extends the accumulation time, and thus limits the number of precursors that can be analyzed per unit of time.

We wrote several data-dependent acquisition (DDA) methods that differed only in reaction and accumulation time. We tested the combinations that were compatible with a total cycle time of less than 500 ms, *i.e.*, to ensure that sufficient MS^1 scans were collected over a chromatographic peak. The LC method consisted of a short, 2.5 minutes reversed-phase LC gradient. The test was done using lipid standards across different classes, injected at a concentration of 2 ng on column for each lipid. To direct the analysis on the fragments that are mostly relevant for identifying the lipids, we relied on the diagnostic fragments that have been described before.[15–18] These include common fragments that are specific for correctly identifying the head group, as well as EIEIO-specific fragments in the glycerol backbone that allow distinguishing the acyl chain at position *sn*-1/3 and *sn*-2 based on the neutral losses. For all compounds of interest, we extracted MS^2 spectrum closest to the chromatographic peak and subsequently extracted the ion counts for all diagnostic fragments. We generated a contour plot of the mean intensity for each diagnostic peak to obtain an overview of the information dependency on reaction and accumulation time.

We present exemplary results for phosphatidylcholine, sphingomyelin, and a triglyceride at the highest tested concentration (Fig. 1; details on the fragments are provided in Fig. S1). In each contour plot, the bottom left edge of the surface indicates the intensity of the diagnostic peak for a single packet of ions at different reaction times. We observe that a short reaction time of 30–60 ms yields more signal for all diagnostic fragments. When the reaction time is 90 ms or longer, the signal decreases by 50–80%. The decrease in fragment intensities could be due to unwanted secondary fragmentation on primary fragments. The intensity of primary fragments generated at shorter reaction times was higher compared to those at longer reaction times, while smaller m/z peaks increased in intensity with longer reaction time. The results show that shorter reaction times are preferable, which is promising for achieving high throughputs. Conversely, we observe the effect of increasing accumulation time and summing multiple packets from bottom to top. The trend aligns with expectations, with a gain that scales with the number of packets. The strongest signals are achieved with the longest accumulation time (200 ms) and the shortest reaction time (30 ms), which corresponds to the summation of six packets and results in a signal amplification of about 3 to 5 times compared to the single-packet method with an accumulation time of 35 ms. The analysis was extended to additional lipids in the test mix (Fig. S2): although the absolute counts vary across lipid and lipid fragments, the trend with decreasing signal at longer reaction times is conserved. We concluded that, in general, the shortest reaction time of 30 ms yields the most diagnostic fragments.

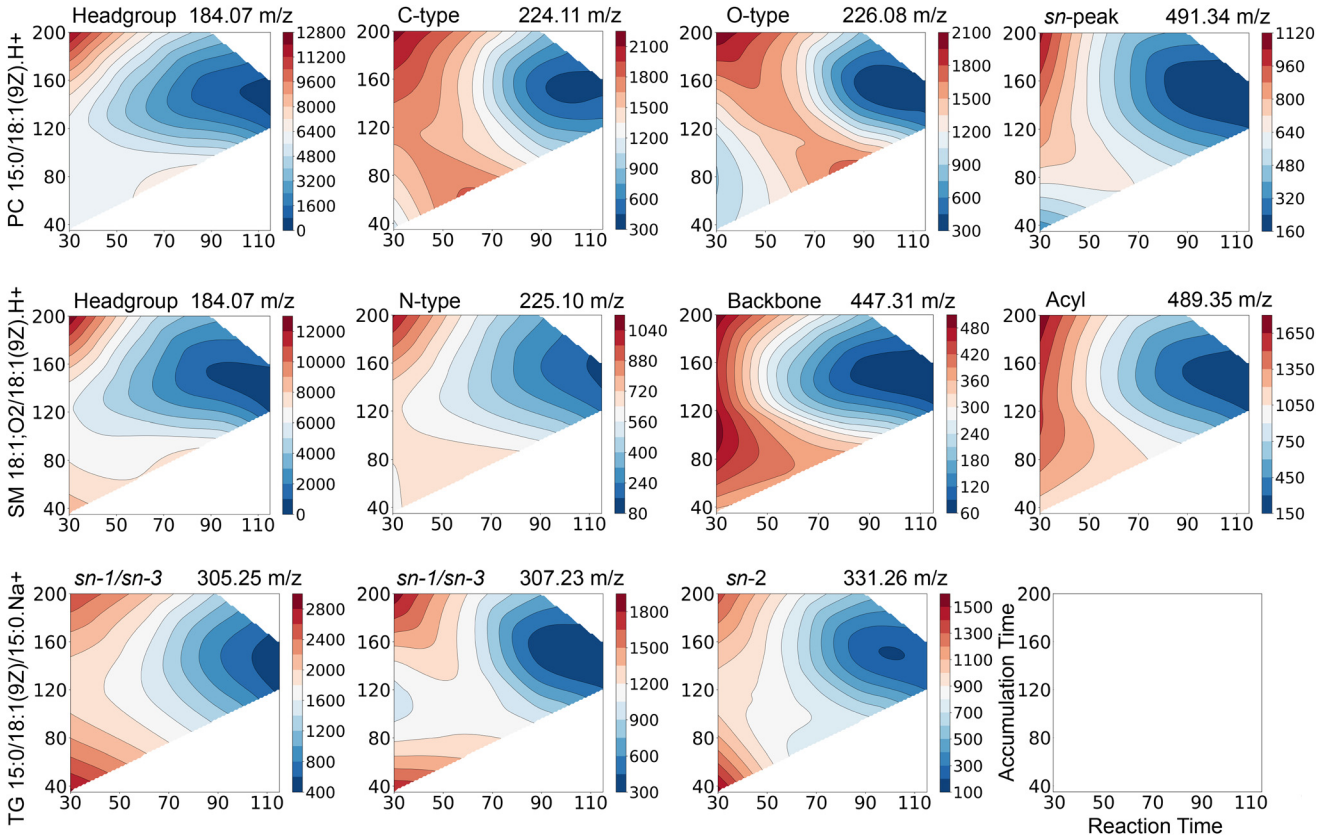

Fig. 1 Intensity of relevant diagnostic peaks of PC 15:0/18:1(9*Z*).H$^+$, SM 18:1;O2/18:1(9*Z*).H$^+$, and TG 15:0/18:1(9*Z*)15:0.Na$^+$. For each tested combination of reaction and accumulation time, we extracted the intensity of the fragment from MS^2 spectrum close to the chromatographic apex and added a smoothed contour plot to visualize the relative trends of the mean intensity. Fragments are selected and named after Baba *et al.*,[18] and indicated in Fig. S1.

Regiospecific fragments

After establishing the optimal settings to obtain the highest counts of diagnostic fragments, we considered the sensitivity. We decided to focus the analysis on the fragments that carry information on *sn*-regioisomerism, because they are not accessible by CID and embody the primary reason for choosing EIEIO. Discrimination of *sn*-1 and *sn*-3 from *sn*-2 is possible when the glycerol backbone fragments between C1 and C2, or C3 and C2 in triglycerides.[15,18] C–C bonds are less prone to breaking compared to ester bonds, which serve as the basis for most other diagnostic fragments. Consequently, detecting fragments that indicate *sn*-regioisomerism becomes more difficult. To estimate the threshold of detection for these fragments across the tested lipids, we analysed varying quantities, ranging from 2 ng to 20 pg on the column, maintaining a reaction time of 30 ms throughout. The accumulation time varied from 35 to 200 ms, which corresponds to one to six packets of ions. For every combination of time and concentration, we measured the intensity of 12 *sn*-specific fragments across eight compounds, and 2 acyl-specific fragments for sphingomyelin and ceramide (Fig. 2). In most instances, the desired fragments were observable at a concentration of 200 pg. Only for [PC 15:0/18:1(9*Z*) + H]$^+$ and [Cer 18:1;O2/15:0 + Na]$^+$ did we detect fragments at an injection of 20 pg. Assuming that the intensity of *sn*-isomer-specific peaks is indicative of their relative concentration, we calculated the regiospecific purity of the standards (Fig. S3). [PC 15:0/18:1(9*Z*) + H]$^+$ was estimated to be ~99% pure, and [PS 15:0/18:1(9*Z*) + H]$^+$ ~100%. The purity of the three PEs ranged from ~86% to ~98%, but the low intensity of the corresponding fragments might bias these results.

Surprisingly, extending the accumulation time beyond 35 ms did not yield any significant benefits. Most signals were stable even as the number of packets increased. We only observed a rise in counts in a few instances, such as with PC 15:0/18:1(9*Z*) (2 ng) or SM 18:1;O2/18:1(9*Z*). While we lack a definitive explanation for the constant fragment yield, we hypothesise that it might result from some form of normalisation included in the spectra acquisition process. Overall, our data indicates that a short reaction time (30 ms) and accumulation time (35 ms) are well-suited to provide a complete characterisation of the tested lipids at a concentration of approximately 200 pg.

The challenge of identifying double bond positions

One significant advantage of EIEIO over CID is its ability to pinpoint the locations of double bonds in unsaturated fatty

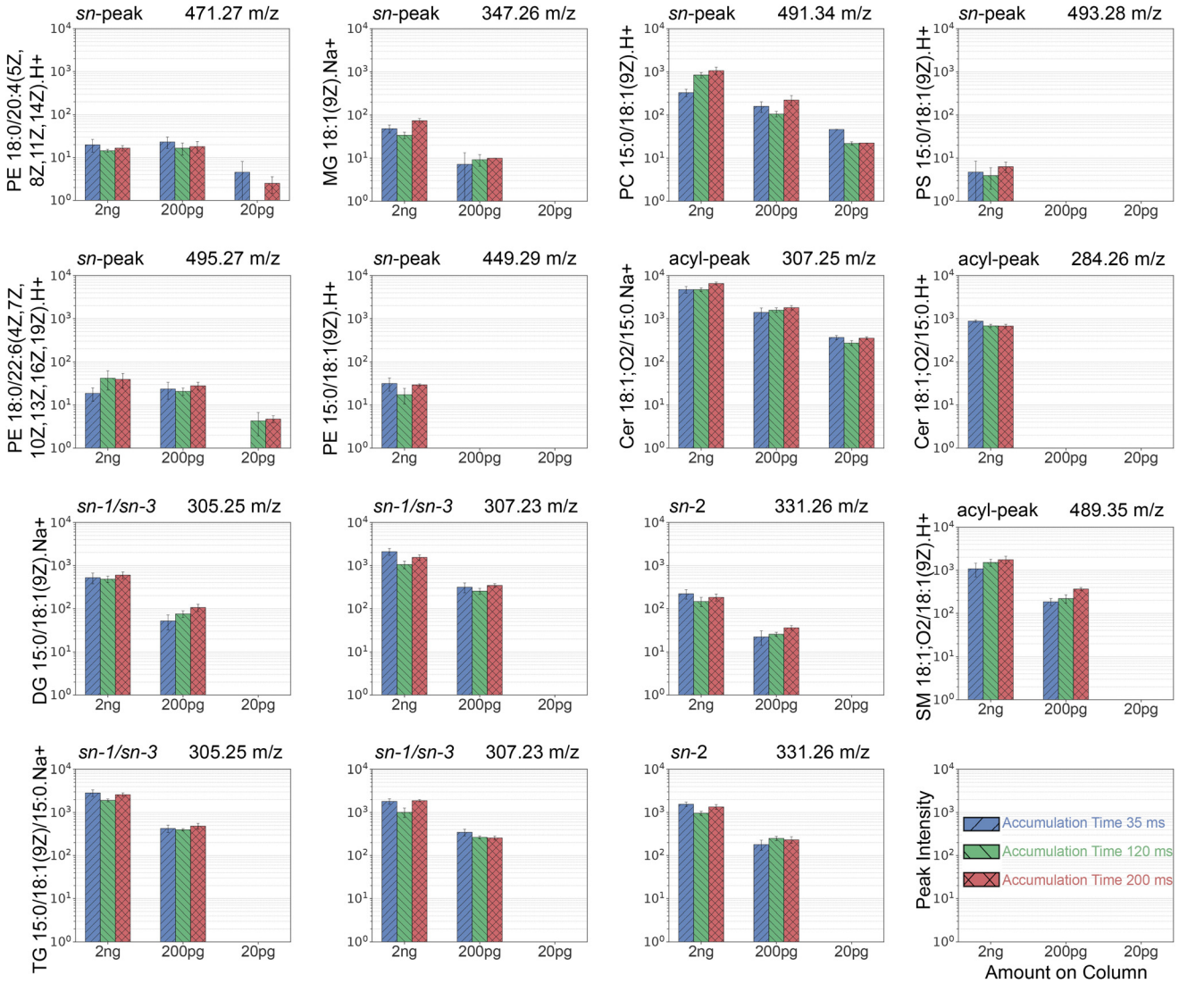

Fig. 2 Concentration dependency of *sn*-specific fragments. In the case of SM 18:1;O2/18:1(9Z) and Cer 18:1;O2/15:0, the fragment is specific for the fatty acyl chain. Missing data indicates that the precursor was not selected for fragmentation by the DDA engine, likely due to its low abundance.

acyl chains.[15] This is feasible because C–C bonds rarely break, allowing for the detection of a series of neutral loss and homolytic radical fragments that shift by 14 Da (–CH_2–) in saturated chains. In theory, a C=C bond causes two successive shifts of 13 Da (–CH–), but it noticeably affects the intensity of nearby fragments. Due to the stronger nature of the double bond (bond dissociation energy ~174 kcal mol^{-1} for C=C in alkenes, compared to 83–90 kcal mol^{-1} for C–C in alkanes or ~92 kcal mol^{-1} for C–O in methanol[22,23]), breaks at the C=C bond is less common and result in lower intensity or even a lack of peaks at the center of the 13 Da shifts. Thankfully, a C=C bond can stabilize the radicals generated from the homolytic break of nearby C–C bonds, leading to enhanced intensity of the related fragments. Thus, the existence of a double bond is represented by a V-shaped fragment intensity pattern. This same pattern is employed for the algorithmic identification of double bonds.[24] A recently presented algorithm seeks shifts of 26 Da at predefined positions, *e.g.* n-3, n-6, n-9, *etc.*[25]

In practice, identifying the C=C positions in EIEIO spectra presents three significant challenges. First, the neutral loss fragments, or the V-shaped intensity pattern, can be hard to detect. In an LC-MS setup, many relevant fragments might be missing or confused with background noise. The second challenge arises because the model for fragment intensity relies on lipids containing single C=C bonds; however, it is still unclear how multiple C=C bonds on the same acyl chain interact or how the initial ester or ether bond affects fragment intensity. Finally, it is understood that heterolytic fragments and hydrogen transfers increase with the electron's kinetic energy.[15] Specifically, H gains result in 13 Da shifts, even in the absence of a C=C bond, highlighting potential bias in their accurate identification.

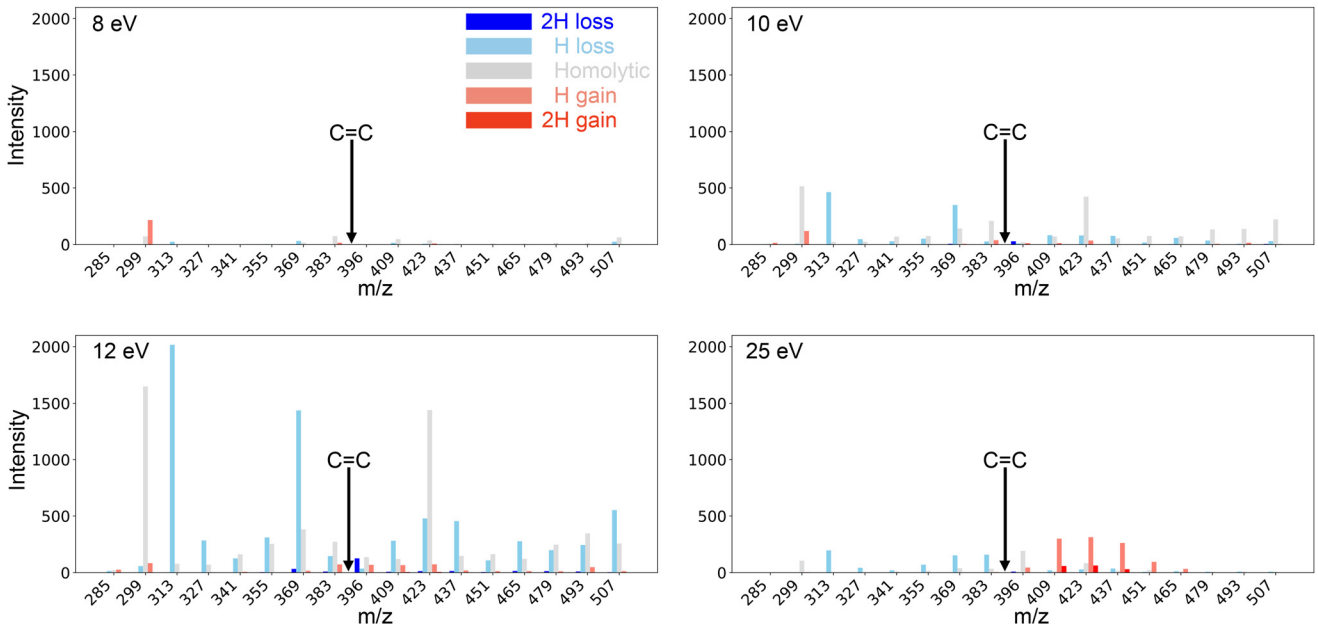

Fig. 3 EIEIO fragments for LPC 0:0/18:1(9*Z*) at increasing electron kinetic energy. The labels on the *x*-axis indicate the *m*/*z* of the expected homolytic fragment, whose intensity is reported in the grey bar. In addition, we report the intensity of hydrogen losses and gains. The arrow indicates the position of the double bond.

We began our analysis by examining the presence of diagnostic and confounding signals in the concentrated 2 ng sample. Based on our earlier findings, we implemented a 30 ms reaction time, along with a total accumulation time of 0.5 s, which we consider the upper limit for LC-MS analysis. To maintain a high abundance of the precursor during the fragmentation period, we switched to a slower, 15-minute gradient. The results for LPC 0:0/18:1(9*Z*) are presented in Fig. 3. A V-shaped pattern around the C=C bond is apparent, but the fragmentation shows significant sensitivity to the electron's kinetic energy. At energies up to 10 eV, the EIEIO spectrum is characterised by homolytic fragments spaced by 14 Da with (grey bars). Hydrogen losses become predominant starting at 12 eV, including the lighter shoulder of the V-shaped pattern (light blue bars). The shift is more prominent for fragments that have lost the C=C, which likely contributes to H retention in the neutral loss. Importantly, the heterolytic H gains appear in fragments near the double bond with as low as 10 eV. These pose the key challenge as they introduce a 13 Da shift, which can lead to the misassignment of the C=C bond by one position, for instance, Δ8 instead of Δ9. At high kinetic energy (25 eV), both single and double hydrogen gains become prevalent for all breakpoints between the C=C bond and the end of the acyl chain, while the distinctive V-shaped pattern fades away. Similarly intricate shifts were noted for other lipids (Fig. S4). In general, hydrogen losses and gains appear to be unavoidable, making them essential to consider when determining C=C bond positions from EIEIO spectra. Since the C=C assignment primarily hinges on the completeness of the fragmentation spectrum, it is critical to pinpoint the conditions that minimize any missing data. Using the same dataset, we examined how the electron kinetic energy affects the intensity of *sn*-specific fragments across all lipid standards (Fig. S5). For most lipids, fragmenting at 12 eV yielded the highest *sn*-specific signal intensity. However, some PE lipids showed slightly higher *sn*-specific intensities at 10 eV. According to our findings, the ideal kinetic energy for detecting carbon double bonds and *sn*-regioisomerism in the examined lipids is approximately 12 eV, as this range yields the highest fragment intensities.

Inference of double-bond positions from LC-MS data

None of the existing EIEIO annotation tools[24,25] are designed to deal with missing values, noisy data, or hydrogen transfers. To fully account for these factors, we adopted a conceptually simple approach that compares the measured spectrum against the simulated EIEIO spectrum of all possible isomers. To simulate EIEIO spectra for any linear unsaturated fatty acid, we first constructed a heuristic model that mimics the fragment intensities in a chain with a single C=C bond (Fig. S6A and B). The model accounts for hydrogen gains and losses as well as intensity shifts based on the distance to the double bond, enabling the simulation of theoretical EIEIO spectra for any unsaturated, linear acyl chain. The model was extended to predict the effect of multiple C=C bonds, which matches favorably with real data EIEIO spectra acquired at long accumulation times (Fig. S6C). We composed an EIEIO neutral loss library for all acyl chains ranging from 4 to 30 carbon atoms, accommodating up to 6 double bonds, including all permutations of non-contiguous C=C positions, for a total of >100 000 fatty acyl chains. We packed the library and annotation routines into LipidOracle, a publicly available container

that conducts in-depth lipid annotation by EIEIO, starting directly from measured MS^2 spectra in MGF format.

We used LipidOracle to quantify the accuracy with which EIEIO spectra identified the correct C=C position in LC-MS experiments. Our initial analysis was conducted using data acquired on a SCIEX 7600 ZenoTOF system, the same instrument used for all previous experiments. We employed a fixed reaction time of 30 ms and a kinetic energy of 12 eV, and wrote multiple methods with accumulation time ranging from 35 to 500 ms. The analysis was extended to a new-generation instrument, the SCIEX 8600 ZenoTOF system, which became available during the review process. The new instrument boasts over ten times higher sensitivity, and we aimed to test whether this enhancement could translate into shorter reaction and accumulation times. Specifically, on the 8600 system, we tested accumulation times ranging from 5 to 65 ms and reaction times ranging from 4 to 30 ms. We injected 2 ng of LPE 18:1(9*Z*), PE 18:0/20:4 (5*Z*,8*Z*,11*Z*,14*Z*), and PE 18:0/22:6(4*Z*,7*Z*,10*Z*,13*Z*,16*Z*,19*Z*) on both instruments. Upon extracting a single MS^2 spectrum closest to the chromatographic centroid, we submitted all spectra to LipidOracle for systematic elucidation of C=C positions. For each experimental spectrum, LipidOracle simulated the EIEIO spectra of all possible isomers, *i.e.*, 16, 1365, and 5005, respectively, and ranked them by a matching score. To account for the potentially ambiguous assignment of double bonds, we retained all isomers with a score within 1% from the top value. Finally, we counted the frequency of correct C=C bond positions in the top isomers identified by LipidOracle, resulting in a true discovery rate (TDR), which indicates the percentage of correct C=C assignments (Fig. 4). For the easiest case of LPE 18:1(9*Z*), the correct double bond position was recovered in all samples except one replicate with 35 ms accumulation time on the ZenoTOF 7600 system, where LipidOracle could not distinguish position 8 and 9. On the 8600 system, instead, the TDR was 100% for all tested settings, including the shortest accumulation time of 5 ms.

Assigning the C=C position is much more challenging for polyunsaturated acyl chains, for glycerophospholipids with two acyl chains because their respective EIEIO fragments overlap confusing the correct recognition of mass shifts. The difficulty increases closer to the head group, because unsaturation affects fewer fragments, and these fragments are further influenced by the head group. In our experiment, the obtained C=C position TDRs for PE 38:4 and PE 40:6 ranged from 75% to 90% for the longest tested accumulation times. The correct isomers PE 18:0/20:4(5*Z*,8*Z*,11*Z*,14*Z*) and PE 18:0/22:6 (4*Z*,7*Z*,10*Z*,13*Z*,16*Z*,19*Z*) were frequently among the top hits, but not the unique ones, explaining the lower TDR. We speculated that the inability to attain 100% TDR for polyunsaturated glycerophospholipids, even with long accumulation times and the most sensitive instrument, reflects a fundamental limit of EIEIO spectral analysis caused by the overlap of homolytic and H-shifted fragments of the two acyl chains. On a positive note, acquisition times of ~15 ms and ~120 ms seem sufficient for capturing the key spectral information on the 8600 and 7600 systems, respectively.

Analysis of complex lipid extracts

Finally, we evaluated the performance of EIEIO in annotating complex lipid extracts in untargeted LC-MS. Our main objective was to apply the optimised workflow and quantify to what extent lipids can be structurally characterised. We analysed liver and plasma extracts on both the 7600 and 8600 systems, using a 15-minute LC gradient with data-dependent acquisition in positive mode only, selecting in each cycle the top 4 precursors for dissociation by EIEIO at 12 eV, with 30 ms reaction time and a total of 200 ms accumulation for each MS^2 spectrum. The total cycle time was ~1 s. After feature detection and deisotoping, MS^2 spectra were exported and analysed with LipidOracle to putatively identify species, chain lengths, *sn*-regioisomerism, and C=C position in unsaturated chains (shown in Fig. 5 for liver and Fig. S7 for plasma). Depending on the fragments detected in an MS^2 spectrum, the annotation can range from species to structural level.

To obtain a summary of the information retrieved for both sample types and instrument, we counted how frequently an MS^2-spectrum included the different classes of diagnostic fragments or was sufficient to infer C=C position (Table 1). The liver extract was more concentrated than the plasma sample, and the newest instrument provided ~30% more MS^2 spectra and ~50% more identifications. Across all experiments, we found fragments indicating the length and saturation of at

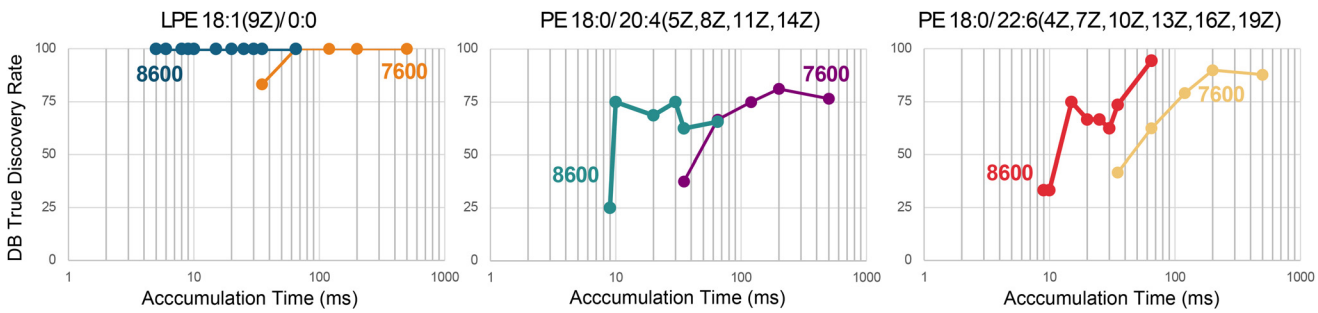

Fig. 4 Double bond identification true discovery rate (TDR) for LPE 0:0/18:1(9*Z*), PE 18:0/20:4(5*Z*,8*Z*,11*Z*,14*Z*), and PE 18:0/22:6 (4*Z*,7*Z*,10*Z*,13*Z*,16*Z*,19*Z*), as quantified by LipidOracle upon testing all theoretical isomers with non-consecutive double bonds. The labels 7600 and 8600 indicate the MS instrument.

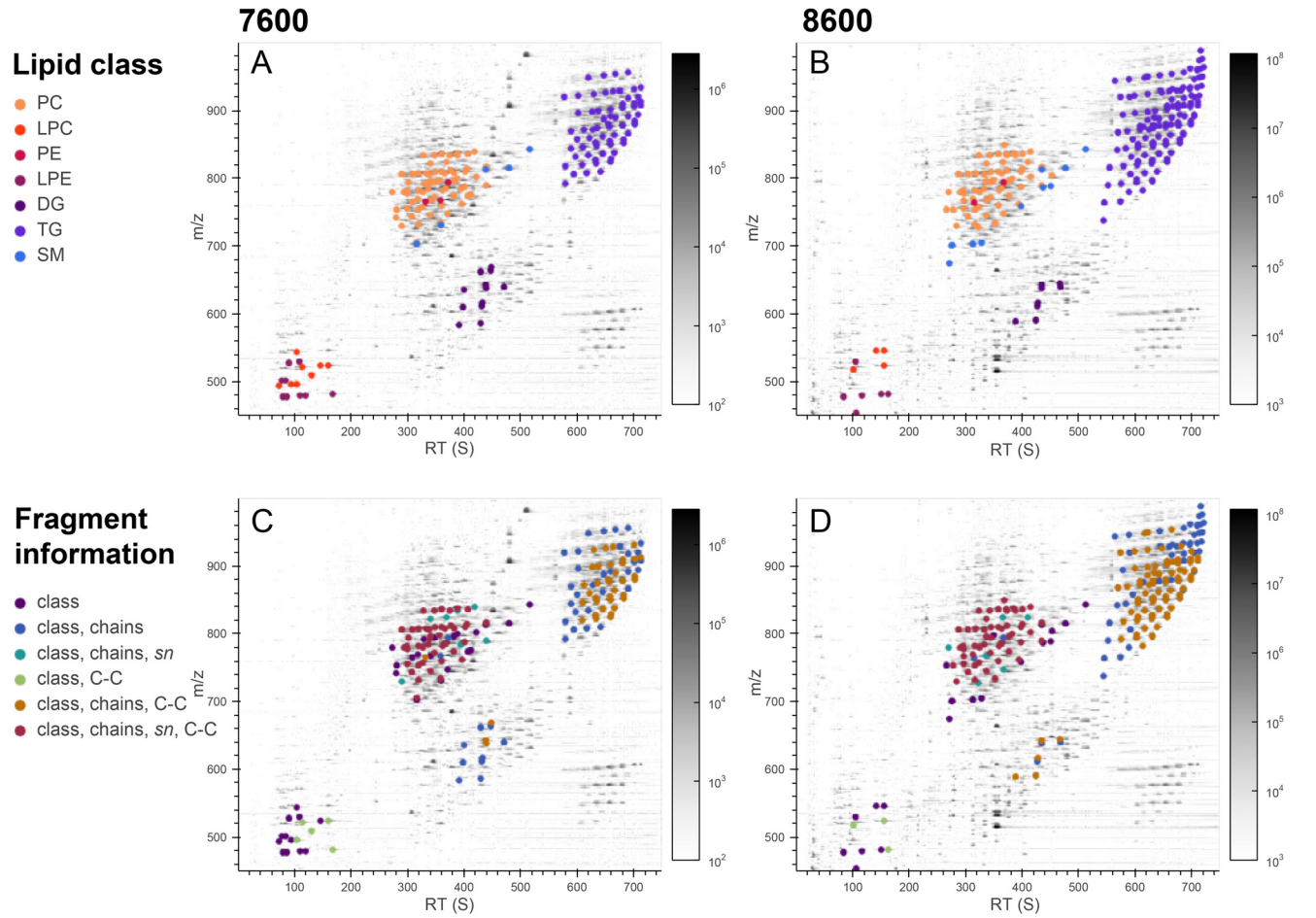

Fig. 5 Annotation of lipid in liver extract by MS^2 spectra collected using either a ZenoTOF 7600 (left column) or a ZenoTOF 8600 system (right column). The upper panels (A and B) report the lipid class. The lower panels (C and D) indicate the type of diagnostic fragments that were matched in the annotation process. *Class* indicates fragments that are related to the head groups, *chains* indicate acyl-specific fragments that enable the definition of length and saturation of one or more fatty acyls, *sn-* indicates that detection of regiospecific fragments, and C–C indicates that the double-bond configuration could be inferred from the EIEIO spectrum and a minimum score of 0.5. In the background, we projected the log10-transformed intensities of MS^1 data.

least one chain in 36–50% of the cases. Regiospecific fragments were detected in ~16–49% of the cases. In about 30% of all identified EIEO spectra, it was possible to infer the position of C=C. In 12–19% of the cases, a single structural isomer stood out in terms of scoring. These included mono- and polyunsaturated lipids such for example, LPC 18:2(9,12)_0:0, LPC 18:1(9)_0:0, PC 16:1(9)/16:0, PC 18:2(9,12)/16:0, PC 16:0/20:4(5,8,11,14), PC 16:0/20:3(8,11,14), PC 18:0/18:2(9,12), PC 18:1(9)/18:0, and PC 18:0/20:4(5,8,11,14), which were detected in liver extracts using the ZenoTOF 7600 system. These results confirm that deep structural characterisation, including *sn*-position and double bond locations in fatty acyl chains, is achievable with an accumulation time of 200 ms.

Conclusions

We demonstrated that comprehensive lipid structural characterisation is achievable on an LC-MS timescale by integrating electron-based fragmentation with fast chromatographic separations using a SCIEX ZenoTOF 7600 system. Optimal EIEIO parameters were identified as an electron kinetic energy of 12 eV, a reaction time of 30 ms, and an accumulation time of 35–200 ms. Even at the shortest accumulation time tested (35 ms), all key diagnostic fragments for lipid class and *sn*-1 position were detectable when injecting ~200 pg lipid standards. Longer accumulation times of up to 200 ms are necessary to identify the position of C=C bonds in acyl chains, especially for polyunsaturated lipids. This step, however, is only possible with approximately 10 times higher lipid concentrations in the range of nanograms on column. Overall, the major outcome of this study is that near-complete lipid structural elucidation by EIEIO is generally feasible within ~0.2 seconds and, thus, well-suited for LC-MS timescales.

From these observations, a two-tiered LC–EIEIO-MS workflow emerges as an effective strategy for lipidomics. For routine analysis, we recommend using 35 ms accumulation time to rapidly profile the lipid constituents and obtain basic

structural annotations (headgroups, chain lengths, and *sn*-linkages). This is sufficient to collect dense MS^2 data by DDA with short LC gradients. For the 2.2 min LC gradient, we routinely adopt for every cycle with subsequent top 7 EIEIO-MS^2 scans of 35 ms each, which provides MS data for up to 1000 precursors per minute. Then, in-depth analysis is best supported by a slower method with EIEIO-MS^2 scans of 200 ms. This can be achieved by several means, such as a fully targeted MS^2 acquisition, a DDA method with an inclusion list, or by re-analysing selected samples with a long LC method. Such a tiered workflow capitalises on EIEIO's strengths for structural lipidomics within practical timeframes and is likely to be broadly applicable in lipidomics studies where large sample sets and detailed structural resolution are both required. If not concerned by throughput, we recommend adopting a single, slower LC-EIEIO-MS method with an accumulation time of at least 200 ms, as we demonstrated with a 15-minute gradient for liver and plasma extracts. Martínez *et al.* reported the analysis of lipids in human plasma by EIEIO using an accumulation time of 1 second;[26] however, our experiments indicate that a longer time has only a marginal effect on the accuracy of annotation.

Despite the clear benefits, there are important practical limitations when deploying EIEIO fragmentation in an LC-MS context. The most critical is the increased complexity of EIEIO spectra due to extensive hydrogen rearrangement reactions that start to emerge at 10 eV and, therefore, are practically unavoidable. These rearrangements lead to fragment mass shifts of ±1 and 2 Da that confound the spectral analysis. We addressed this challenge by incorporating hydrogen shifts and considering all possible C=C isomers in LipidOracle. This allowed for inferring the position and confidence of carbon double bonds, even in cases of noisy and partial spectra. Our systematic analysis also highlighted that for largely polyunsaturated lipids, it remains prohibitive to reduce the false discovery rate below 20%. Our experiments demonstrate that the accuracy of C=C localisation doesn't improve with longer accumulation times or with the new ZenoTOF 8600 system, which offers >10× increased sensitivity. Hence, we believe that the performance is limited by the overlap of homo- and hydrogen-shifted fragments originating from multiple chains. Our current EIEIO-fragmentation model is based on simple heuristic rules that don't allow for accurately predicting intensities for polyunsaturated chains. Hence, we adopted a scoring scheme that weights the presence of matching fragments more heavily and the guessed intensity less. To improve the structural identification of polyunsaturated glycerides and phospholipids, a more accurate prediction of fragment intensities is needed to adopt a stricter matching metric.

Conflicts of interest

The authors declare no competing financial interest.

Data availability

Raw data, extracted spectra in MGF format, and results are available at https://doi.org/10.3929/ethz-b-000734594. LipidOracle is accessible at https://hub.docker.com/r/zamboni-lab/lipidoracle.

Supplementary information (SI) is available. See DOI: https://doi.org/10.1039/d5an00567a.

Acknowledgements

This work was supported by the ETH Research Commission and by grants from the Strategic Focal Area Personalized Health and Related Technologies (PHRT) of the ETH Domain (Grants #504 and #603).

References

1 M. R. Wenk, The Emerging Field of Lipidomics, *Nat. Rev. Drug Discovery*, 2005, **4**(7), 594–610, DOI: 10.1038/nrd1776.
2 M. Li, L. Yang, Y. Bai and H. Liu, Analytical Methods in Lipidomics and Their Applications, *Anal. Chem.*, 2014, **86**(1), 161–175, DOI: 10.1021/ac403554h.
3 G. van Meer, Cellular Lipidomics, *EMBO J.*, 2005, **24**(18), 3159–3165, DOI: 10.1038/sj.emboj.7600798.
4 I. Y. Dobrosotskaya, A. C. Seegmiller, M. S. Brown, J. L. Goldstein and R. B. Rawson, Regulation of SREBP Processing and Membrane Lipid Production by Phospholipids in Drosophila, *Science*, 2002, **296**(5569), 879–883, DOI: 10.1126/science.1071124.
5 W. Zhang, R. Jian, J. Zhao, Y. Liu and Y. Xia, Deep-Lipidotyping by Mass Spectrometry: Recent Technical Advances and Applications, *J. Lipid Res.*, 2022, **63**(7), 100219, DOI: 10.1016/j.jlr.2022.100219.
6 H. Ren, A. Triebl, S. Muralidharan, M. R. Wenk, Y. Xia and F. Torta, Mapping the Distribution of Double Bond Location Isomers in Lipids across Mouse Tissues, *Analyst*, 2021, **146**(12), 3899–3907, DOI: 10.1039/D1AN00449B.
7 X. Ma and Y. Xia, Pinpointing Double Bonds in Lipids by Paternò-Büchi Reactions and Mass Spectrometry, *Angew. Chem., Int. Ed.*, 2014, **53**(10), 2592–2596, DOI: 10.1002/anie.201310699.
8 G. Feng, M. Gao, R. Fu, Q. Wan, T. Wang, Z. Zhang and S. Chen, Direct N-Me Aziridination Reaction Enables Pinpointing C=C Bonds in Lipids with Mass Spectrometry. bioRxiv April 25, 2022, p 2022.04.24.489320.DOI: 10.1101/2022.04.24.489320.
9 E. Hirtzel, M. Edwards, D. Freitas, Z. Liu, F. Wang and X. Yan, Aziridination-Assisted Mass Spectrometry of Nonpolar Sterol Lipids with Isomeric Resolution, *J. Am. Soc. Mass Spectrom.*, 2023, **34**(9), 1998–2005, DOI: 10.1021/jasms.3c00161.
10 M. C. Thomas, T. W. Mitchell, D. G. Harman, J. M. Deeley, J. R. Nealon and S. J. Blanksby, Ozone-Induced

Dissociation: Elucidation of Double Bond Position within Mass-Selected Lipid Ions, *Anal. Chem.*, 2008, **80**(1), 303–311, DOI: 10.1021/ac7017684.

11 B. L. J. Poad, X. Zheng, T. W. Mitchell, R. D. Smith, E. S. Baker and S. J. Blanksby, Online Ozonolysis Combined with Ion Mobility-Mass Spectrometry Provides a New Platform for Lipid Isomer Analyses, *Anal. Chem.*, 2018, **90**(2), 1292–1300, DOI: 10.1021/acs.analchem.7b04091.

12 H. Takeda, M. Okamoto, H. Takahashi, B. Buyantogtokh, N. Kishi, H. Okano, H. Kamiguchi and H. Tsugawa, Dual Fragmentation via Collision-Induced and Oxygen Attachment Dissociations Using Water and Its Radicals for C=C Position-Resolved Lipidomics, *Commun. Chem.*, 2025, **8**(1), 148, DOI: 10.1038/s42004-025-01525-y.

13 H. Takahashi, Y. Shimabukuro, D. Asakawa, S. Yamauchi, S. Sekiya, S. Iwamoto, M. Wada and K. Tanaka, Structural Analysis of Phospholipid Using Hydrogen Abstraction Dissociation and Oxygen Attachment Dissociation in Tandem Mass Spectrometry, *Anal. Chem.*, 2018, **90**(12), 7230–7238, DOI: 10.1021/acs.analchem.8b00322.

14 P. E. Williams, D. R. Klein, S. M. Greer and J. S. Brodbelt, Pinpointing Double Bond and Sn-Positions in Glycerophospholipids via Hybrid 193 Nm Ultraviolet Photodissociation (UVPD) Mass Spectrometry, *J. Am. Chem. Soc.*, 2017, **139**(44), 15681–15690, DOI: 10.1021/jacs.7b06416.

15 J. L. Campbell and T. Baba, Near-Complete Structural Characterization of Phosphatidylcholines Using Electron Impact Excitation of Ions from Organics, *Anal. Chem.*, 2015, **87**(11), 5837–5845, DOI: 10.1021/acs.analchem.5b01460.

16 T. Baba, J. L. Campbell, J. C. Y. Le Blanc and P. R. S. Baker, In-Depth Sphingomyelin Characterization Using Electron Impact Excitation of Ions from Organics and Mass Spectrometry[S], *J. Lipid Res.*, 2016, **57**(5), 858–867, DOI: 10.1194/jlr.M067199.

17 T. Baba, J. L. Campbell, J. C. Y. Le Blanc and P. R. S. Baker, Structural Identification of Triacylglycerol Isomers Using Electron Impact Excitation of Ions from Organics (EIEIO), *J. Lipid Res.*, 2016, **57**(11), 2015–2027, DOI: 10.1194/jlr.M070177.

18 T. Baba, J. L. Campbell, J. C. Y. Le Blanc, P. R. S. Baker and K. Ikeda, Quantitative Structural Multiclass Lipidomics Using Differential Mobility: Electron Impact Excitation of Ions from Organics (EIEIO) Mass Spectrometry, *J. Lipid Res.*, 2018, **59**(5), 910–919, DOI: 10.1194/jlr.D083261.

19 T. Baba, P. Ryumin, E. Duchoslav, K. Chen, A. Chelur, B. Loyd and I. Chernushevich, Dissociation of Biomolecules by an Intense Low-Energy Electron Beam in a High Sensitivity Time-of-Flight Mass Spectrometer, *J. Am. Soc. Mass Spectrom.*, 2021, **32**(8), 1964–1975, DOI: 10.1021/jasms.0c00425.

20 G. Liebisch, E. Fahy, J. Aoki, E. A. Dennis, T. Durand, C. S. Ejsing, M. Fedorova, I. Feussner, W. J. Griffiths, H. Köfeler, A. H. Merrill, R. C. Murphy, V. B. O'Donnell, O. Oskolkova, S. Subramaniam, M. J. O. Wakelam and F. Spener, Update on LIPID MAPS Classification, Nomenclature, and Shorthand Notation for MS-Derived Lipid Structures, *J. Lipid Res.*, 2020, **61**(12), 1539–1555, DOI: 10.1194/jlr.S120001025.

21 A. Delabriere, P. Warmer, V. Brennsteiner and N. Zamboni, SLAW: A Scalable and Self-Optimizing Processing Workflow for Untargeted LC-MS, *Anal. Chem.*, 2021, **93**(45), 15024–15032, DOI: 10.1021/acs.analchem.1c02687.

22 S. J. Blanksby and G. B. Ellison, Bond Dissociation Energies of Organic Molecules, *Acc. Chem. Res.*, 2003, **36**(4), 255–263, DOI: 10.1021/ar020230d.

23 R. G. Bergman and A. Streitwieser, *Table Of Organic Bond Dissociation Energies* 2018.

24 H. Takeda, Y. Matsuzawa, M. Takeuchi, M. Takahashi, K. Nishida, T. Harayama, Y. Todoroki, K. Shimizu, N. Sakamoto, T. Oka, M. Maekawa, M. H. Chung, Y. Kurizaki, S. Kiuchi, K. Tokiyoshi, B. Buyantogtokh, M. Kurata, A. Kvasnička, U. Takeda, H. Uchino, M. Hasegawa, J. Miyamoto, K. Tanabe, S. Takeda, T. Mori, R. Kumakubo, T. Tanaka, T. Yoshino, M. Okamoto, H. Takahashi, M. Arita and H. Tsugawa, MS-DIAL, 5 Multimodal Mass Spectrometry Data Mining Unveils Lipidome Complexities, *Nat. Commun.*, 2024, **15**(1), 9903, DOI: 10.1038/s41467-024-54137-w.

25 Y. Chen, J. Yang, X. Wang, Y. Zhang, Y. Shao, H. Li, X. Dong, F. Jiang, C. Hu and G. Xu, Structural Annotation Method for Locating Sn- and C=C Positions of Lipids Using Liquid Chromatography–Electron Impact Excitation of Ions from Organics (EIEIO)–Mass Spectrometry, *Anal. Chem.*, 2025, **97**(9), 4998–5007, DOI: 10.1021/acs.analchem.4c05560.

26 S. Martínez, A. Gradillas, H. Cermakova, M. Witting and C. Barbas, Determining Carbon-Carbon Double Bond Position of Unsaturated Glycerophospholipids in Human Plasma NIST® SRM® 1950 by Electron Impact Excitation of Ions from Organics-Tandem Mass Spectrometry (EIEIO-MS/MS), *J. Pharm. Biomed. Anal.*, 2025, **266**, 117081, DOI: 10.1016/j.jpba.2025.117081.